



Article

A Hybridized Method for Temporal Variable-Order Fractional Partial Differential Equations with Fractional Laplace Operator

Chengyi Wang ¹ and Shichao Yi ^{1,2,*} ¹ School of Science, Jiangsu University of Science and Technology, Zhenjiang 212003, China; cywang@just.edu.cn² Yangzijiang Shipbuilding Group, Taizhou 212299, China

* Correspondence: shichaoyi@just.edu.cn

Abstract: In this paper, we present a more general approach based on a Picard integral scheme for nonlinear partial differential equations with a variable time-fractional derivative of order $\alpha(\mathbf{x}, t) \in (1, 2)$ and space-fractional order $s \in (0, 1)$, where $v = u'(t)$ is introduced as the new unknown function and u is recovered using the quadrature. In order to get rid of the constraints of traditional plans considering the half-time situation, integration by parts and the regularity process are introduced on the variable v . The convergence order can reach $O(\tau^2 + h^2)$, different from the common $L_{1,2-\alpha}$ schemes with convergence rate $O(\tau^{2,3-\alpha(\mathbf{x},t)})$ under the infinite norm. In each integer time step, the stability, solvability and convergence of this scheme are proved. Several error results and convergence rates are calculated using numerical simulations to evidence the theoretical values of the proposed method.

Keywords: time–space fractional advection–diffusion equation; variable fractional order; nonlinearity; stability; second order



Citation: Wang, C.; Yi, S. A Hybridized Method for Temporal Variable-Order Fractional Partial Differential Equations with Fractional Laplace Operator. *Fractal Fract.* **2024**, *8*, 105. <https://doi.org/10.3390/fractalfract8020105>

Academic Editor: Agnieszka B. Malinowska

Received: 5 December 2023

Revised: 13 January 2024

Accepted: 16 January 2024

Published: 8 February 2024



Copyright: © 2024 by the authors. Licensee MDPI, Basel, Switzerland. This article is an open access article distributed under the terms and conditions of the Creative Commons Attribution (CC BY) license (<https://creativecommons.org/licenses/by/4.0/>).

1. Introduction

One of the most useful and applicable generalizations of the ordinary derivatives of integer orders and integrals is the fractional calculus. Utilizing the models based on derivatives of fractional orders in several branches of science and engineering is a major study of many mathematicians and physicists [1–4]. Fractional partial differential equations (FPDEs), particularly space- and time-fractional equations, have been widely studied to demonstrate the existence of solutions and the validity of these problems [5–7].

In this paper, we will consider the nonlinear multi-dimensional fractional advection–diffusion equation involving variable time–space orders.

$${}^c \mathfrak{D}_t^{\alpha(\mathbf{x},t)} (1 + (-\Delta)^s) u(\mathbf{x}, t) + A(\mathbf{x}, t) ((-\Delta)^s - \Delta) u(\mathbf{x}, t) = \mathcal{N}(u(\mathbf{x}, t)) + f(\mathbf{x}, t), \quad (1)$$

with the following initial and boundary conditions:

$$\begin{aligned} u(\mathbf{x}, t) &= 0, \mathbf{x} \in \partial\Omega, t \in (0, T], \\ u(\mathbf{x}, 0) &= u_0(\mathbf{x}), u_t(\mathbf{x}, 0) = v_0(\mathbf{x}), \mathbf{x} \in \Omega. \end{aligned} \quad (2)$$

In addition, finding reliable and powerful numerical and analytical methods for solving FPDEs has been focused on in the last two decades. According to the mathematical literature, fractional partial differential equations have been progressed in various problems in science and engineering such as the Schrödinger, diffusion and telegraph fractional equations [5,8–12].

Nonetheless, the analytical solutions for the majority of fractional partial differential equations remain elusive. Consequently, over the past two decades, a significant portion of researchers has concentrated on approximations and numerical methods for tackling these fractional-order systems. Many researchers have particularly emphasized

difference schemes, given their superior stability and solvability compared to alternative approaches. For example, Adomian decomposition method (ADM) was utilized to approximate the time–space FPDE with the Caputo sense in [13]. The space–time fractional advection–diffusion equations are linear partial pseudo-differential equations with Feller space-fractional differentiation derivatives and are used to model transport at the earth’s surface in [14]. The space–time fractional diffusion equation with Caputo time-fractional derivative α and Riesz–Feller space-fractional derivative β is studied in [15], and the convergence rate is $O(\tau^{3-\alpha} + h^{3-\beta})$. In [16], multi-dimensional space–time variable-order fractional Schrödinger equations are introduced with a Caputo time-fractional derivative and Riesz–Feller space-fractional derivative. The time–space fractional telegraph equation with local fractional derivatives is investigated in [17]. Among them, the fractional advection–diffusion equation, as an important model, has been widely studied in engineering applications and fast calculations. In [18], the fractional advection–diffusion equation model is a new approach to describe the vertical distribution of suspended sediment concentration in steady turbulent flow. Gu has successively published multiple outstanding achievements in rapid calculation in [19–21].

The foundational time model, tailored for discrete schemes, often requires the incorporation of half-time steps for the variable u due to their suitability in representing derivatives and integration processes. Conversely, conventional energy methods for u typically involve its coupling with the variable v . In [22], we pivot our focus to primarily address the situation of v . We meticulously establish the system’s stability and solvability and demonstrate that the convergence of u is of second order. It is worth noting that the derivative operation is inherently unbounded, whereas integration acts as a refining operator. In Section 4 of this paper, we substantiate the effectiveness of the integral formula when coupled with the difference scheme, illustrating its robust stability.

2. Preliminaries and Some Lemmas

Consider the set $\{t_n | n \geq 0\}$, which comprises uniformly spaced time intervals with $t_n = n\tau$ and $\tau > 0$. Suppose

$$u_i^n = u_i^{n-1} + \tau(v_i^{n-1} + v_i^n)/2, \quad (3)$$

$$\int_0^\tau g(\eta) \frac{\partial v_i}{\partial \eta} d\eta = \left[\frac{v_i^1 - v_i^0}{\tau} \int_0^\tau g(\eta) d\eta \right], \quad (4)$$

$$\begin{aligned} \int_{t_{n-1}}^{t_n} g(\eta) \frac{\partial v_i}{\partial \eta} d\eta &= \left[\int_{t_{n-1}}^{t_n} (\eta - (t_{n-1} + t_{n-2})) g(\eta) d\eta \right] \frac{v_i^n}{\tau^2} \\ &\quad - \left[\int_{t_{n-1}}^{t_n} (\eta - (t_n + t_{n-2})) g(\eta) d\eta \right] \frac{2v_i^{n-1}}{\tau^2} \\ &\quad + \left[\int_{t_{n-1}}^{t_n} (\eta - (t_n + t_{n-1})) g(\eta) d\eta \right] \frac{v_i^{n-2}}{\tau^2}, \quad (n \geq 2), \end{aligned} \quad (5)$$

where u_i^n and v_i^n correspond to the function values and their respective first derivative values at time t_n for the point x_i , while $g(t)$ represents a smooth function defined within the interval $(0, T]$.

Here is the difference scheme we will explore for Equation (1):

Case I: $n = 1$

$$\begin{aligned} &\frac{1}{\tau\Gamma(2-\alpha)} [a_0^1 v_i^1 - a_1^1 v_i^0] + \frac{1}{\tau\Gamma(2-\alpha)} [a_0^1 (-\Delta)^s v_i^1 - a_1^1 (-\Delta)^s v_i^0] \\ &= -\tau A_i^1 [(-\Delta)^s - \Delta] \left(\frac{v_i^0 + v_i^1}{2} \right) + \mathcal{N}(u_i^0) + F_i^1, \end{aligned} \quad (6)$$

Case II: $n \geq 2$

$$\begin{aligned} & \frac{1}{\tau\Gamma(2-\alpha)} \left[a_0^n v_i^n - \sum_{k=1}^{n-1} a_{(n-k)}^n v_i^k - a_n^n v_i^0 \right] \\ & + \frac{1}{\tau\Gamma(2-\alpha)} \left[a_0^n (-\Delta)^s v_i^n - \sum_{k=1}^{n-1} a_{(n-k)}^n (-\Delta)^s v_i^k - a_n^n (-\Delta)^s v_i^0 \right] \\ & = -\tau A_i^n [(-\Delta)^s - \Delta] \left(\frac{v_i^{n-1} + v_i^n}{2} \right) + 2\mathcal{N}(u_i^{n-1}) - \mathcal{N}(u_i^{n-2}) + F_i^n, \end{aligned} \quad (7)$$

where

$$\begin{aligned} a_l^n &= a_l(t_n) = \int_{t_i}^{t_{l+1}} \frac{dt}{t^{\alpha(t_n)-1}} = \frac{1}{2-\alpha(t_n)} \left[(t_{l+1})^{2-\alpha(t_n)} - (t_l)^{2-\alpha(t_n)} \right] \\ &= \frac{\tau^{3-\alpha(t_n)}}{2-\alpha(t_n)} \left[(l+1)^{2-\alpha(t_n)} - l^{2-\alpha(t_n)} \right], l \geq 0. \end{aligned} \quad (8)$$

and

$$F_i^n = -A_i^n [(-\Delta)^s - \Delta] u_i^{n-1} + f_i^n.$$

A_i^n corresponds to the variable coefficients $A(\mathbf{x}, t)$ at the point (\mathbf{x}_i, t_n) . It is verified that $\{a_0^n, a_1^n, a_2^n, a_3^n, \dots, a_{n-1}^n\}$ constitutes a monotonically decreasing sequence for each value of n with

$$a_0^n = a_0(t_n) = \tau^{2-\alpha(t_n)} / (2-\alpha(t_n)). \quad (9)$$

2.1. Time-Discretization of the Present Scheme

To establish the time-fractional derivation in the current scheme, the following lemmas are required.

Lemma 1. For any $v = \{v(t_0), v(t_1), v(t_2), \dots\}$, we have

$$\begin{aligned} & \sum_{n=1}^N \left[a_0^n v_i^n - \sum_{k=1}^{n-1} a_{(n-k)}^n v_i^k - a_n^n v_i^0 \right] v(t_n) \\ & \geq \frac{t_m^{1-\alpha(t_n)} \tau}{2} \sum_{n=1}^N v(t_n)^2 - \frac{t_N^{2-\alpha(t_n)} v(t_0)^2}{2(2-\alpha(t_n))}. \end{aligned} \quad (10)$$

where $a_l(t_n)$ is defined in (8).

Proof.

$$\begin{aligned} & \sum_{n=1}^N \left[a_0^n v_i^n - \sum_{k=1}^{n-1} a_{(n-k)}^n v_i^k - a_n^n v_i^0 \right] v(t_n) \\ &= \sum_{n=1}^N a_0^n v(t_n)^2 - \sum_{n=1}^N \sum_{k=1}^{n-1} a_{(n-k)}^n v_i^k v(t_n) - \sum_{n=1}^N a_{(n-1)}^n v(t_0) v(t_n) \\ &\geq \sum_{n=1}^N a_0^n v(t_n)^2 - \frac{1}{2} \sum_{n=1}^N \sum_{k=1}^{n-1} a_{(n-k)}^n (v(t_k)^2 + v(t_n)^2) - \frac{1}{2} \sum_{n=1}^N a_{(n-1)}^n (v(t_0)^2 + v(t_n)^2) \\ &= \sum_{n=1}^N a_0^n v(t_n)^2 - \frac{1}{2} \sum_{n=1}^N \sum_{k=1}^{n-1} (a_{(n-k-1)}^n - a_{(n-k)}^n) v(t_k)^2 - \frac{1}{2} \sum_{n=1}^N \sum_{k=1}^{n-1} (a_{(n-k-1)}^n - a_{(n-k)}^n) v(t_n)^2 \\ &\quad - \frac{1}{2} \sum_{n=1}^N a_{(n-1)}^n v(t_0)^2 - \frac{1}{2} \sum_{n=1}^N a_{(n-1)}^n v(t_n)^2 \end{aligned} \quad (11)$$

By rearranging the order of summation, we have

$$\begin{aligned}
 & \sum_{n=1}^N \left[a_0^n v(t_n) - \sum_{k=1}^{n-1} (a_{(n-k-1)}^n - a_{(n-k)}^n) v(t_k) - a_{(n-1)}^n v(t_0) \right] v(t_n) \\
 & \geq \sum_{n=1}^N a_0^n v(t_n)^2 - \frac{1}{2} \sum_{n=2}^N (a_0^n - a_{(n-1)}^n) v(t_n)^2 - \frac{1}{2} \sum_{k=1}^{N-1} (a_0^n - a_{(n-k)}^n) v(t_k)^2 \\
 & \quad - \frac{1}{2} \sum_{n=1}^N a_{(n-1)}^n v(t_0)^2 - \frac{1}{2} \sum_{n=1}^N a_{(n-1)}^n v(t_n)^2 + \sum_{n=1}^N (a_2^n - a_2^{n*}) v_i^{n-2} v(t_n) \\
 & = \frac{1}{2} \sum_{n=1}^N a_{N-n}(t_n) v(t_n)^2 - \frac{1}{2} \sum_{n=1}^N a_{(n-1)}^n v(t_0)^2 \\
 & \geq \frac{1}{2} a_{N-1} \sum_{n=1}^N v(t_n)^2 - \frac{(t_N^{2-\alpha} + \tau^{2-\alpha})}{2(2-\alpha)} v(t_0)^2 \\
 & \geq \frac{1}{8} t_N^{1-\alpha} \tau \sum_{n=1}^N v(t_n)^2 - \frac{(t_N^{2-\alpha} + \tau^{2-\alpha})}{2(2-\alpha)} v(t_0)^2
 \end{aligned} \tag{12}$$

where

$$\begin{aligned}
 \sum_{n=1}^N a_{n-1}(t_n) & \leq \sum_{n=0}^{N-1} a_n(t_n) = \int_{t_0}^{t_N} \frac{d\zeta}{\zeta^{\alpha(t_n)-1}} \leq \frac{t_N^{2-\alpha(t_n)}}{2-\alpha(t_n)} + \frac{\tau^{2-\alpha(t_n)}}{2-\alpha(t_n)}, \\
 a_l & \geq a_{n-1} = \frac{1}{4} \int_{t_{l-1}}^{t_l} \zeta^{1-\alpha(t_n)} d\zeta \geq \frac{t_{l+1}^{1-\alpha(t_n)}}{4} \tau \quad (0 \leq l \leq n-1).
 \end{aligned} \tag{13}$$

Obviously, α is the largest number in the series $\alpha(t_n)$ in the formula of a_l^n , and the same procedure may be easily adapted to obtain corresponding behaviours for b_l^n . \square

Lemma 2. Assume $v(t) \in C^2[0, t_n]$. We obtain

$$\begin{aligned}
 & \left| \int_0^{t_n} v'(t) \frac{dt}{(t_n - t)^{\alpha(t_n)-1}} - \frac{1}{\tau} \left[a_0^n v_i^n - \sum_{k=1}^{n-1} a_{(n-k)}^n v_i^k - a_n^n v_i^0 \right] \right| \\
 & \leq \frac{4\tau^2 t_n^{2-\alpha(t_n)}}{3(2-\alpha(t_n))} \|v'''(t)\|_{L^\infty([0, t_n])},
 \end{aligned} \tag{14}$$

where a_l^n is defined in (8), $1 < \alpha(t_n) < 2$ and $n > 1$.

Proof. Obviously, it suffices to verify

$$\begin{aligned}
 & \sum_{k=1}^n \left[\int_{t_{k-1}}^{t_k} (\eta - (t_{k-1} + t_{k-2})) g(\eta) d\eta \right] v_i^k - 2 \left[\int_{t_{k-1}}^{t_k} (\eta - (t_k + t_{k-2})) g(\eta) d\eta \right] v_i^{k-1} \\
 & + \left[\int_{t_{k-1}}^{t_k} (\eta - (t_k + t_{k-1})) g(\eta) d\eta \right] v_i^{k-2} \\
 & = \frac{1}{\tau} \left[a_0^n v_i^n - \sum_{k=1}^{n-1} a_{(n-k)}^n v_i^k - a_n^n v_i^0 \right].
 \end{aligned} \tag{15}$$

Combining this with the result of Lemma 1, we obtain

$$\begin{aligned}
 & \left| \int_0^{t_n} v'(t) \frac{dt}{(t_n - t)^{\alpha(t_n)-1}} - \frac{1}{\tau} \left[a_0^n v_i^n - \sum_{k=1}^{n-1} a_{(n-k)}^n v_i^k - a_n^n v_i^0 \right] \right| \\
 &= \left| \sum_{k=1}^n \int_{t_{k-1}}^{t_k} \left[v(t) - \left(L_{(k-2)} v(t_{k-2}) + L_{(k-1)} v(t_{k-1}) + L_k v(t_k) \right) \right]' \frac{dt}{(t_n - t)^{\alpha(t_n)-1}} \right| \\
 &= \sum_{k=1}^n \int_{t_{k-1}}^{t_k} \left| \left[(t - t^k)^3 / 6 \max\{|v'''(t)|\}_{t \in [t_{k-2}, t_k]} \right]' \right| \frac{dt}{(t_n - t)^{\alpha(t_n)-1}} \\
 &\leq \frac{4\tau^2}{3} \sum_{k=1}^n \int_{t_{k-1}}^{t_k} \frac{\|v'''(t)\|_{L^\infty([t_{k-2}, t_k])} dt}{(t_n - t)^{\alpha(t_n)-1}} \leq \frac{4\tau^2 t_n^{2-\alpha(t_n)}}{3(2 - \alpha(t_n))} \|v'''(t)\|_{L^\infty([0, t_n])},
 \end{aligned} \tag{16}$$

where $L_{(k-2)}, L_{(k-1)}, L_k$ are the Lagrange interpolation functions on the nodes $t_{(k-2)}, t_{(k-1)}, t_k$. This completes the proof. \square

2.2. Semi-Discretization in Space of the Present Scheme

Denote

$$(-\Delta)u(t) = \Delta_c u(t),$$

where Δ_c is a differential matrix format of the Laplace operator $(-\Delta)$. Then the matrix representation of the operator $(-\Delta)^s$ can be given by Δ_c^s . Thus, we use the finite-difference approximation of $(-\Delta)^s$:

$$(-\Delta)^s u(t) = \Delta_c^s u(t)$$

For functions $\epsilon(x)$ on Ω , we use the 2-norm with

$$\|\epsilon(\mathbf{x})\|_\infty = \max_{\mathbf{x}_i \in \Omega} \{|\epsilon(\mathbf{x}_i)|\}, \|\epsilon(\mathbf{x})\|_{0,h} = \left(h^d \sum_{\mathbf{x}_i \in \Omega} \{\epsilon(\mathbf{x}_i)^2\} \right)^{1/2}.$$

Due to the similarity of the 2-norm, we will use the $\|\cdot\|_\infty$ format to replace the above norm for convenience in the following process. And we obtain the approximate error of the difference representation under this norm.

From the differential discretization scheme, we have the approximate property of the matrix Δ_c . Assuming that $u \in C^4(\Omega)$, we obtain

$$\|(-\Delta)u - \Delta_c u\|_\infty \leq h^2 \|u\|_{C^4},$$

which for $u = \phi_j$ with $(-\Delta)u = (-\Delta)\phi_j = \lambda_j \phi_j$ gives

$$\|(\lambda_j I - \Delta_c)\phi_j\|_\infty \leq h^2 \|\phi_j\|_{C^4}.$$

Theorem 1. *If $u \in C^4(\Omega)$, the following error estimate holds:*

$$\|(-\Delta)^s u - \Delta_c^s u_h\|_\infty \leq C(s, u, d, \Delta_c) h^2,$$

where Ω is a nonempty open bounded set with Lipschitz continuous boundaries, and $C(s, u, d, \Delta_c)$ is a constant number depending on u, s, d and Δ_c .

Proof. We decompose the left-hand side of the error estimate as

$$\|(-\Delta)^s u - \Delta_c^s u_h\|_\infty \leq \|(-\Delta)^s u - \Delta_c^s u\|_\infty + \|\Delta_c^s u - \Delta_c^s u_h\|_\infty. \tag{17}$$

Firstly, we estimate the first term. Using the notation $K_0 = \min\{\lambda_1, \lambda_{1,h}\}$, we have $\max\left\{\left|1 - \frac{\lambda_j}{K}\right|, \left\|I - \frac{\Delta_c}{K}\right\|\right\} = 1 - \frac{K_0}{K}$. We obtain that

$$\begin{aligned}
 & \|(-\Delta)^s u - \mathbf{B}^s u\|_\infty \\
 &= \|K^s \sum_{k=0}^\infty \binom{s}{k} (-1)^k \sum_{j=1}^\infty \left(1 - \frac{\lambda_j}{K}\right)^k u_j \phi_j - K^s \sum_{k=0}^\infty \binom{s}{k} (-1)^k \sum_{j=1}^\infty \left(I_h - \frac{\Delta_c}{K}\right)^k u_j \phi_j\|_\infty \\
 &= K^s \left\| \sum_{k=1}^\infty \binom{s}{k} (-1)^k \sum_{j=1}^\infty \left[\left(I_h - \frac{\lambda_j I_h}{K}\right)^k - \left(I_h - \frac{\Delta_c}{K}\right)^k \right] u_j \phi_j \right\|_\infty \\
 &\leq K^s \sum_{k=1}^\infty \binom{s}{k} (-1)^{k-1} \left\| \sum_{j=1}^\infty \left[\left(I_h - \frac{\lambda_j I_h}{K}\right)^{k-1} + \dots + \left(I_h - \frac{\Delta_c}{K}\right)^{k-1} \right] \left[\frac{\lambda_j I_h - \Delta_c}{K} \right] u_j \phi_j \right\|_\infty \\
 &\leq s K^{s-1} \sum_{k=1}^\infty \binom{s-1}{k-1} (-1)^{k-1} \sum_{j=1}^\infty k * \max\left\{\left|1 - \frac{\lambda_j}{K}\right|, \left\|I - \frac{\Delta_c}{K}\right\|\right\} \left\| (\lambda_j I_h - \Delta_c) u_j \phi_j \right\|_\infty \tag{18} \\
 &\leq s K^{s-1} \sum_{k=1}^\infty \binom{s-1}{k-1} (-1)^{k-1} \sum_{j=1}^\infty \left(1 - \frac{K_0}{K}\right)^{k-1} \left\| (\lambda_j I_h - \Delta_c) u_j \phi_j \right\|_\infty \\
 &\leq s K^{s-1} \sum_{k=0}^\infty \binom{s-1}{k} (-1)^k \left(1 - \frac{K_0}{K}\right)^k \sum_{j=1}^\infty \left\| (\lambda_j I_h - \Delta_c) u_j \phi_j \right\|_\infty \\
 &\leq s K^{s-1} \left(\frac{K_0}{K}\right)^{s-1} \sum_{j=1}^\infty \left\| (\lambda_j I_h - \Delta_c) u_j \phi_j \right\|_\infty \\
 &\leq \lambda_1^{s-1} \sum_{j=1}^\infty \left\| (\lambda_j I_h - \Delta_c) u_j \phi_j \right\|_\infty.
 \end{aligned}$$

The last is the estimate of $\sum_{j=1}^\infty \left\| (\lambda_j I_h - \Delta_c) u_j \phi_j \right\|_\infty$,

$$\sum_{j=1}^\infty \left\| (\lambda_j I_h - \Delta_c) u_j \phi_j \right\|_\infty \leq \sum_{j=1}^\infty u_j h^2 \|\phi_j\|_{H^6(\Omega)} \leq \sum_{j=1}^\infty u_j h^2 \lambda_j^3 \leq h^2 \sum_{j=1}^\infty u_j j^{\frac{6}{d}}. \tag{19}$$

Considering the boundedness of $\sum_{j=1}^\infty u_j j^{\frac{6}{d}}$,

$$\sum_{j=1}^\infty \left\| (\lambda_j I_h - \Delta_c) u_j \phi_j \right\|_\infty \leq C_I h^2. \tag{20}$$

Taking (20) into (18), we obtain the estimate

$$\|(-\Delta)^s u - \Delta_c^s u\|_\infty \leq C_I \lambda_1^{s-1} h^2. \tag{21}$$

Secondly, we estimate the second term,

$$\|\Delta_c^s u - \Delta_c^s u_h\|_\infty \leq \|\Delta_c^s\|_\infty \|u - u_h\|_\infty. \tag{22}$$

From the property of the difference matrix Δ_c , we have $\|\Delta_c^s\|_\infty \leq 4d$. Then,

$$\|\Delta_c^s u - \Delta_c^s u_h\|_\infty \leq 4d \|u - u_h\|_\infty \leq 4d h^2 \|u\|_{C^2}. \tag{23}$$

Finally, inserting the inequalities into each other implies the following error estimate:

$$\|(-\Delta)^s u - \Delta_c^s u_h\|_\infty \leq \left(4d \|u\|_{C^2} + C_{II} \lambda_1^{s-1}\right) h^2 = C(s, u, d, \Delta_c) h^2. \tag{24}$$

□

2.3. Analysis of the Time–Space Discretization of the Present Scheme

Based on Lemma 2 and Equations (6) and (7), we have

$$\begin{aligned}
 {}^c\mathcal{D}_0^{\alpha(t)}u(x,t) &= \frac{1}{\Gamma(2-\alpha(t_n))} \int_0^{t_n} \frac{\partial^2 u(x,t)}{\partial t^2} \frac{dt}{(t_n-t)^{\alpha(t_n)-1}}, \\
 &= \frac{1}{\tau\Gamma(2-\alpha(t_n))} \left[a_0^n v_i^n - \sum_{k=1}^{n-1} a_{(n-k)}^n v_i^k - a_n^n v_i^0 \right] + (r_1)_i^n,
 \end{aligned}
 \tag{25}$$

and

$$(-\Delta)^s u_i^n = \mathbf{B}^s(i, :)\mathbf{u}^n + (r_2)_i^n := (-\Delta)_c^s u_i^n + (r_2)_i^n,
 \tag{26}$$

where

$$|(r_1)_i^n| \leq c_1 \tau^2, |(r_2)_i^n| \leq c_2 (\tau^2 + h^2).
 \tag{27}$$

Taking into account the distinct characteristics of the nonlinear part $\mathcal{N}u(\mathbf{x}, t)$,

$$\mathcal{N}u^n(\mathbf{x}, t) = cc2\mathcal{N}u^{n-1}(\mathbf{x}, t) - \mathcal{N}u^{n-2}(\mathbf{x}, t) + c_3\tau^2, \quad n \geq 2.
 \tag{28}$$

When the above results are substituted into (1), the following is obtained:

$$\begin{aligned}
 &\frac{1}{\tau\Gamma(2-\alpha)} (1 - (-\Delta)_c^s) \left[a_0^n v_i^n - \sum_{k=1}^{n-1} a_{(n-k)}^n v_i^k - a_n^n v_i^0 \right] \\
 &= -\tau A_i^n ((-\Delta)_c^s - \Delta) \left(\sum_{k=1}^{n-1} v_i^k + \frac{v_i^0 + v_i^n}{2} \right) + \hat{F}_i^n + R_i^n,
 \end{aligned}
 \tag{29}$$

where

$$|R_i^n| \leq C(\tau^2 + h^2),
 \tag{30}$$

and \hat{F}_i^n involves the original F_i^n and the approximate value of $\mathcal{N}u(\mathbf{x}, t)$.

We also define

$$\|g^n\|_\infty = \max_{1 \leq i \leq m} |g_i^n|, \|g^n\| = \sqrt{\mathfrak{m}_i \sum_{i=1}^m (g_i^n)^2},
 \tag{31}$$

where D is the metric coefficient of Ω . Moreover, when $g(\Gamma) = 0$, it is observed that:

$$\|g^n\|_\infty \leq \frac{\sqrt{D}}{2} |\nabla g^n|, |\nabla g_i^n| \leq D |g_i^n|.
 \tag{32}$$

3. Main Results

In this section, the solvability, stability and convergence of this scheme are proved. The notation for the inner product discretization form is used as follows:

$$(u, w) = \int_\Omega u w d\Omega = \sum_{i=1}^m \mathfrak{w}_i (u_i w_i), \forall u_i, w_i \in L^2(\Omega),
 \tag{33}$$

where \mathfrak{w}_i is described as the Gauss weight at the point x_i . Subsequently, some lemmas are introduced.

Lemma 3. Let $0 \leq s \leq 1$ and $f, (-\Delta)^s f \in L^p$. Then, for any arbitrary $p \geq 1$, there holds

$$\int |f|^{p-2} f (-\Delta)^s f dx \geq \frac{2}{p} \int ((-\Delta)^{s/2} |f|^{p/2})^2 dx.$$

Lemma 4. Suppose $\{v^n\}$ is the solution of

$$\begin{aligned} & \frac{1}{\tau\Gamma(2-\alpha(t_n))} (1 - (-\Delta)_c^s) \left[a_0^n v_i^n - \sum_{k=1}^{n-1} a_{(n-k)}^n v_i^k - a_n^n v_i^0 \right] \\ & = -\tau A_i^n ((-\Delta)_c^s - \Delta) \left(\sum_{k=1}^{n-1} v_i^k + \frac{v_i^0 + v_i^n}{2} \right) + R_i^n, u_i^n(\partial\Omega) = 0, i = 1, 2, 3, \dots, m, n = 1, 2, 3, \dots \end{aligned} \tag{34}$$

We have

$$\sum_{n=1}^N \|\nabla u^n\|^2 \leq \sum_{n=1}^N \|\nabla u^0\|^2 + \frac{t_N^{2-\alpha}}{\hat{A}\tau^2\Gamma(3-\alpha)} (\|v^0\|^2 + \|(-\Delta)_c^{s/2}|v^0|\|^2) + \frac{\Gamma(2-\alpha)t_N^{\alpha-1}}{\hat{B}\tau} \sum_{n=1}^N \|R^n\|^2, \tag{35}$$

with $A_i^n \geq \hat{A} > 0$.

Proof. Summing i and n from 1 to m and from 1 to N by multiplying both sides of (34) with w_i , the following is obtained:

$$\begin{aligned} & \frac{1}{\tau\Gamma(2-\alpha)} \sum_{i=1}^m \left\{ \sum_{n=1}^N w_i \left((1 + (-\Delta)_c^s) \left[a_0^n v_i^n - \sum_{k=1}^{n-1} a_{(n-k)}^n v_i^k - a_n^n v_i^0 \right] \right) v_i^n \right\} \\ & = - \sum_{n=1}^N \sum_{i=1}^m \left(A_i^n w_i \left[\sum_{x \in \mathbf{x}} (-\Delta)_c^s \left(\sum_{k=1}^{n-1} v^k + \frac{v^0 + v^n}{2} \right) \right] v_i^n \right) \\ & + \sum_{n=1}^N \sum_{i=1}^m \left(A_i^n w_i \left[\sum_{x \in \mathbf{x}} \Delta \left(\sum_{k=1}^{n-1} v^k + \frac{v^0 + v^n}{2} \right) \right] v_i^n \right) + \sum_{n=1}^N \sum_{i=1}^m w_i R_i^n v_i^n. \end{aligned} \tag{36}$$

Using Lemma 1, we have

$$\begin{aligned} & \frac{1}{\tau\Gamma(2-\alpha)} \sum_{n=1}^N \sum_{i=1}^m \left(w_i \left[a_0^n v_i^n - \sum_{k=1}^{n-1} a_{(n-k)}^n v_i^k - a_n^n v_i^0 \right] v_i^n \right) \\ & \geq \frac{1}{2\Gamma(2-\alpha)} t_N^{1-\alpha} \sum_{n=1}^N \|v^n\|^2 - \frac{t_N^{2-\alpha}}{2\tau\Gamma(3-\alpha)} \|v^0\|^2, \end{aligned} \tag{37}$$

$$\begin{aligned} & \frac{1}{\tau\Gamma(2-\alpha)} \sum_{n=1}^N \sum_{i=1}^m \left(w_i (-\Delta)_c^s \left[a_0^n v_i^n - \sum_{k=1}^{n-1} a_{(n-k)}^n v_i^k - a_n^n v_i^0 \right] v_i^n \right) \\ & \geq \frac{1}{2\Gamma(2-\alpha)} t_N^{1-\alpha} \sum_{n=1}^N \|(-\Delta)_c^{s/2}|v^n|\|^2 - \frac{t_N^{2-\alpha}}{2\tau\Gamma(3-\alpha)} \|(-\Delta)_c^{s/2}|v^0|\|^2, \end{aligned} \tag{38}$$

and

$$\begin{aligned} & \frac{1}{\tau\Gamma(2-\alpha)} \sum_{n=1}^N \sum_{i=1}^m \left(w_i \Delta \left[a_0 v_i^n - \sum_{k=1}^{n-1} (a_{n-k-1} - a_{n-k}) v_i^k - a_{n-1} v_i^0 \right] v_i^n \right) \\ & \geq \frac{1}{2\Gamma(2-\alpha)} t_N^{1-\alpha} \sum_{n=1}^N \|\nabla v^n\|^2 - \frac{t_N^{2-\alpha}}{2\tau\Gamma(3-\alpha)} \|\nabla v^0\|^2. \end{aligned} \tag{39}$$

When the boundary conditions in (34) are applied, it results in $v_i^n(\partial\Omega) = 0$. Consequently,

$$\begin{aligned} & -\tau \sum_{i=1}^m \left(w_i (-\Delta)_c^s \left(\sum_{k=1}^{n-1} v_i^k + \frac{v_i^0 + v_i^n}{2} \right) v_i^n \right) \\ & = -\tau \sum_{i=1}^m \left(w_i (-\Delta)_c^s \left(\sum_{k=1}^{n-1} v_i^k + \frac{v_i^0 + v_i^n}{2} \right) v_i^n \right) = -\frac{\tau}{2} \sum_{k=1}^n (-\Delta)_c^{s/2} |v^k|^2, \\ & \tau \sum_{i=1}^m \left(w_i \Delta \left(\sum_{k=1}^{n-1} v_i^k + \frac{v_i^0 + v_i^n}{2} \right) v_i^n \right) \\ & = -\tau \sum_{i=1}^m \left(w_i \Delta \left(\sum_{k=1}^{n-1} v_i^k + \frac{v_i^0 + v_i^n}{2} \right) v_i^n \right) = -\frac{\tau}{2} \sum_{k=1}^n \|\nabla v^k\|^2. \end{aligned} \tag{40}$$

In addition,

$$\sum_{n=1}^N \sum_{i=1}^m \mathfrak{w}_i R_i^n v_i^n \leq \frac{1}{2} \frac{1}{\Gamma(2-\alpha)} t_N^{1-\alpha} \sum_{n=1}^N \|v^n\|^2 + \frac{\Gamma(2-\alpha)}{2} t_N^{\alpha-1} \sum_{n=1}^N \|R^n\|^2. \tag{41}$$

Substituting (37)–(41) into (36), we obtain

$$\begin{aligned} & \frac{1}{2\Gamma(2-\alpha)} t_N^{1-\alpha} \sum_{n=1}^N \|v^n\|^2 - \frac{t_N^{2-\alpha}}{2\tau\Gamma(3-\alpha)} \sum_{n=1}^N \|v^0\|^2 + \frac{1}{2\Gamma(2-\alpha)} t_N^{1-\alpha} \sum_{n=1}^N \|(-\Delta)_c^{s/2} |v^n|\|^2 \\ & - \frac{t_N^{2-\alpha}}{2\tau\Gamma(3-\alpha)} \sum_{n=1}^N \|(-\Delta)_c^{s/2} |v^0|\|^2 \\ & \leq -\frac{\tau\hat{A}}{2} \sum_{n=1}^N \left\| \sum_{k=1}^n (-\Delta)_c^{s/2} |v^k| \right\|^2 - \frac{\tau\hat{A}}{2} \sum_{n=1}^N \left\| \sum_{k=1}^n \nabla v^k \right\|^2 + \frac{1}{2\Gamma(2-\alpha)} t_N^{1-\alpha} \sum_{n=1}^N \|v^n\|^2 \\ & + \frac{\Gamma(2-\alpha)}{2} t_N^{\alpha-1} \sum_{n=1}^N \|R^n\|^2. \end{aligned} \tag{42}$$

Then,

$$\sum_{n=1}^N \left\| \sum_{k=1}^n \nabla v^k \right\|^2 \leq \frac{t_N^{2-\alpha}}{\hat{A}\tau^2\Gamma(3-\alpha)} \left(\|v^0\|^2 + \|(-\Delta)_c^{s/2} |v^0|\|^2 \right) + \frac{\Gamma(2-\alpha)t_N^{\alpha-1}}{\hat{A}\tau} \sum_{n=1}^N \|R^n\|^2. \tag{43}$$

Replacing v with u in (43), the ensuing inequality is derived:

$$\begin{aligned} \sum_{n=1}^N \|\nabla |u^n|\|^2 & \leq \sum_{n=1}^N \|\nabla u^0\|^2 + \left(\frac{\tau}{2}\right)^2 \sum_{n=1}^N \left\| \sum_{k=1}^n \nabla v^k \right\|^2 \\ & \leq \sum_{n=1}^N \|\nabla u^0\|^2 + \frac{t_N^{2-\alpha}}{\hat{A}\tau^2\Gamma(3-\alpha)} \left(\|v^0\|^2 + \|(-\Delta)_c^{s/2} |v^0|\|^2 \right) + \frac{\Gamma(2-\alpha)t_N^{\alpha-1}}{\hat{A}\tau} \sum_{n=1}^N \|R^n\|^2. \end{aligned} \tag{44}$$

□

Theorem 2. Uniqueness in solvability is achieved by the difference scheme (6) and (7).

Proof. As (6) and (7) constitute the linear algebraic equations at different time t_i , it is sufficient for the corresponding homogeneous equations to be demonstrated:

$$\begin{aligned} & \frac{1}{\tau\Gamma(2-\alpha)} (1 - (-\Delta)_c^s) \left[a_0^n v(t_n) - \sum_{k=1}^{n-1} (a_{(n-k-1)}^n - a_{(n-k)}^n) v(t_k) - a_{(n-1)}^n v(t_0) \right] \\ & = \tau A_i^n (-\Delta)_c^s \left(\sum_{k=1}^{n-1} v_i^k + \frac{v_i^0 + v_i^n}{2} \right) + \tau B_i^n \Delta \left(\sum_{k=1}^{n-1} v_i^k + \frac{v_i^0 + v_i^n}{2} \right), \\ & u_i^n(\Gamma) = 0, 1 \leq i \leq m, n \geq 1. \end{aligned} \tag{45}$$

Only a zero solution is attainable. Through the utilization of Lemma 4, the following is derived:

$$\|\nabla u^n\| = 0, n = 1, \dots, N.$$

Combining the boundary conditions in (2), we obtain

$$u_i^n = v_i^n = 0, n \geq 1, 1 \leq i \leq m.$$

This completes the proof. □

Theorem 3. Let $u(x, t)$ and $v(x, t)$ be the solution of (6) and (7). Then, the following inequality holds:

$$\|u(x_i, t_n) - u_i^n\|_\infty \leq \tilde{C}\tilde{D}\sqrt{\Gamma(2-\alpha)\Gamma^\alpha(\tau^2 + h^2)},$$

where \tilde{C}, \tilde{D} represent constant numbers.

Proof. Denote

$$\begin{aligned}\hat{v}_i^n &= v(\mathbf{x}_i, t_n) - v_i^n, \\ \hat{u}_i^n &= u(\mathbf{x}_i, t_n) - u_i^n, n \geq 0\end{aligned}\quad (46)$$

Subtracting (6) and (7) from (29) and (30), respectively, the error equations are encountered:

$$\begin{aligned}& \frac{1}{\tau\Gamma(2-\alpha)}(1 - (-\Delta)_c^s) \left[a_0^n \hat{v}(t_n) - \sum_{k=1}^{n-1} (a_{(n-k-1)}^n - a_{(n-k)}^n) \hat{v}(t_k) - a_{(n-1)}^n \hat{v}(t_0) \right] \\ &= \tau A_i^n (-\Delta)_c^s \left(\sum_{k=1}^{n-1} \hat{v}_i^k + \frac{\hat{v}_i^0 + \hat{v}_i^n}{2} \right) + \tau B_i^n \Delta \left(\sum_{k=1}^{n-1} v_i^k + \frac{v_i^0 + v_i^n}{2} \right), \hat{u}_i^n(\Gamma) = \hat{v}_i^n(\Gamma) = 0, n \geq 1.\end{aligned}\quad (47)$$

Using Lemma 4, we have

$$\|\nabla \hat{u}^n\|^2 \leq \frac{\Gamma(2-\alpha)t_n^{\alpha-1}}{4\hat{C}} \tau \sum_{k=1}^n \|R^k\|^2, \tau < n\tau \leq T. \quad (48)$$

Taking into account (29) and (31), the following is obtained:

$$|\nabla \hat{u}^n| \leq \tilde{c} \sqrt{\frac{D\Gamma(2-\alpha)T^\alpha}{4\hat{C}} (\tau^2 + h^2)}, \tau < n\tau \leq T. \quad (49)$$

The result is obtained by observing (32):

$$\|\hat{u}^n\|_\infty \leq \tilde{C}\tilde{D} \sqrt{\Gamma(2-\alpha)T^\alpha (\tau^2 + h^2)}, \tau < n\tau \leq T. \quad (50)$$

where \tilde{C}, \tilde{D} represent constant numbers, completing the proof. \square

4. Numerical Experiments

In this section, some experiments showcase the effectiveness of the current scheme.

4.1. One-Dimensional Space-Fractional Laplace Case

Consider the following problem:

$$\begin{aligned}& {}_0^c \mathfrak{D}_t^{\alpha(x,t)} (1 + (-\Delta)^s u(x,t)) + A(x,t)((-\Delta)^s - \Delta)u(x,t) = u^2(x,t) + f(x,t), (x,t) \in (0,1) \times (0,1], \\ & u(x,0) = \sin(\pi t); u(0,t) = u(1,t) = 0, t \in (0,1].\end{aligned}\quad (51)$$

The exact solution of the system is

$$u(x,t) = t^{k+\frac{5}{4}} \sin(\pi x), \quad (52)$$

with

$$\alpha(x,t) = \frac{5}{4} + \frac{1}{2} \sin(x) \sin(t). \quad (53)$$

In Figure 1, the upper two figures depict the present solutions for this nonlinear system at $s = 0.3$ (upper left) and $s = 0.7$ (upper right), with $h = 1/32$, $\tau = 1/10$ and $k = 2$. According to the exact solutions on the lower left and the values of u with different t with $s = 0.3$ (the circle represents the analytical solution and the asterisk represents the numerical solution), the present scheme is very accurate. Figure 2 displays the curves of the present scheme and the exact solutions at the boundary line ($x = 0.5, t = 0.4$) for $s = 0.6$ and $k = 2, 3$. It can be observed from these figures that the proposed methods effectively match the analytical solution.

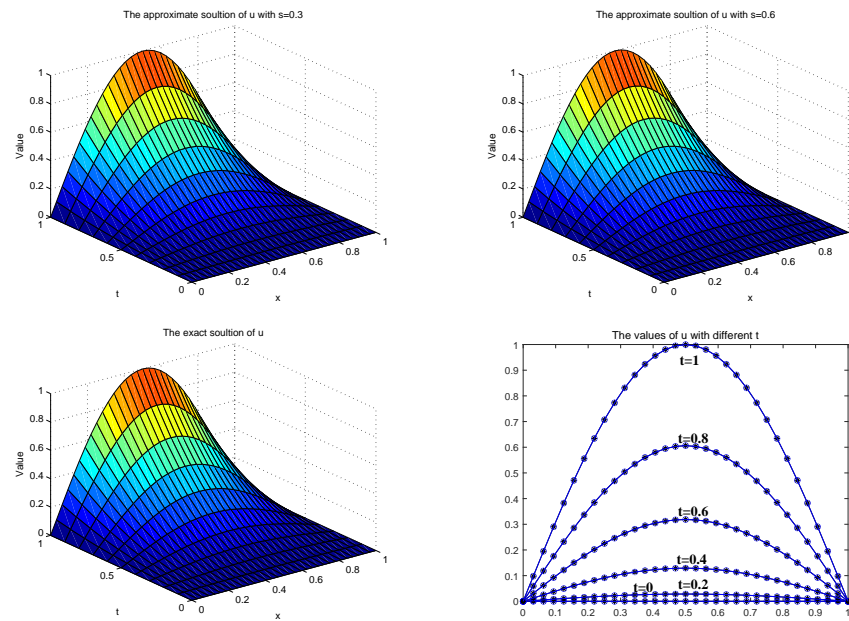


Figure 1. The curved surfaces for the present numerical scheme (upper), the exact solution (lower left), and the values of u with different t with $s = 0.3$ (lower right).

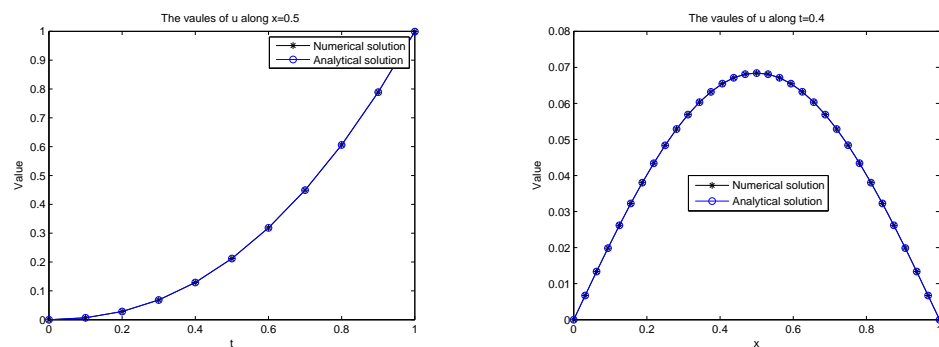


Figure 2. The curves of the present numerical scheme (asterisk) and the analytical solution (circle) with $x = 0.5$ (left) and $t = 0.4$ (right).

Taking s as 0.2, 0.6, Figure 3 represents temporal convergence curves for different values of the parameter with $h = 1/2056$. From it, we have the conclusion that the space scheme is convergent and the slopes of the two convergence curves are close to 2.

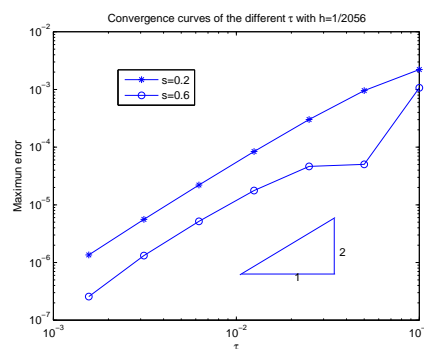


Figure 3. The curves of the present numerical scheme (asterisk) and the analytical solution (circle).

Table 1 displays the present space convergence orders at $t = 1$, which are close to our theoretical values $O(h^2)$.

Table 1. Space convergence situation ($\tau = 1/1000$).

h	1/8	1/16	1/32	1/64	1/128	1/256
$k = 2, s = 0.65$						
Error	8.7888×10^{-3}	2.1888×10^{-3}	5.4653×10^{-4}	1.3644×10^{-4}	3.3945×10^{-5}	8.3243×10^{-6}
Order		2.0055	2.0018	2.0021	2.0070	2.0278
$k = 3, s = 0.75$						
Error	1.0329×10^{-2}	2.5707×10^{-3}	6.4201×10^{-4}	1.6051×10^{-4}	4.0172×10^{-5}	1.0091×10^{-5}
Order		2.0065	2.0015	2.0000	1.9984	1.9931

4.2. Two-Dimensional Space-Fractional Laplace Case

To assess the numerical effectiveness, the following two-dimensional numerical experiment is considered:

$$\begin{aligned}
 & {}_0^c \mathcal{D}_t^{\alpha(t)} (1 + (-\Delta)^s u(x, y, t)) + A(x, y, t)((-\Delta)^s - \Delta)u(x, y, t) \\
 & = 2u(x, y, t) - u^2(x, y, t) + f(x, y, t), (x, y) \in (0, 1)^2, t \in (0, 1],
 \end{aligned}
 \tag{54}$$

with the boundary conditions

$$u(x, y, 0) = 0; u(\partial\Omega, t) = 0, t \in (0, 1].
 \tag{55}$$

The equation’s exact solution is as follows:

$$u(x, y, t) = \exp(t) \sin(2\pi x) \sin(2\pi y)
 \tag{56}$$

with

$$\alpha(t) = \alpha_0 + \frac{1}{4}t.$$

With $\tau = 1/1000$ and $s = 0.4, 0.7$, the maximum errors considered for different space mesh sizes at $t = 1$ are provided in Table 2. From this table, the temporal convergence order is close to $O(\tau^2)$. This result demonstrates the robust stability of this scheme.

Table 2. The maximum errors and the corresponding spatial order at $t = 1$.

τ	1/8	1/16	1/32	1/64	1/128
$s = 0.4$					
Error	1.0479×10^{-1}	2.5846×10^{-2}	6.4394×10^{-3}	1.6078×10^{-3}	4.0182×10^{-4}
Order		2.0195	2.0050	2.0018	2.0005
$s = 0.7$					
Error	6.4704×10^{-2}	1.5905×10^{-2}	3.9593×10^{-3}	9.8852×10^{-4}	2.4705×10^{-4}
Order		2.0244	2.0061	2.0019	2.0005

In Figure 4, the curved surfaces of the present numerical scheme (left) and the analytical solution (right) are depicted, with $h_x = h_y = 1/32$, $\tau = 1/10$, $\alpha = 1.4$ and $s = 0.7$ at $t = 1$. It is evident that the numerical solutions closely approximate the analytical solutions.

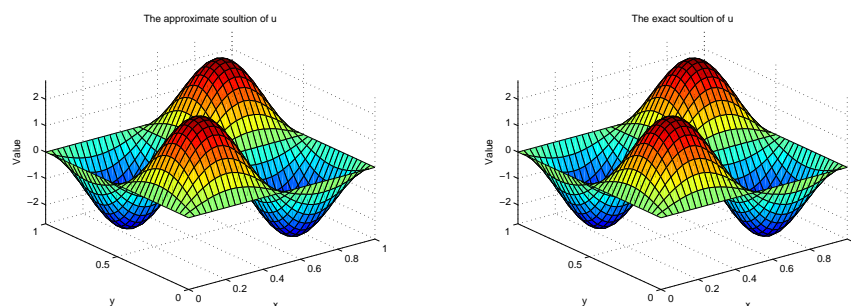


Figure 4. The surface of the numerical solution (left) and the exact solution (right) for $s = 0.7$ and $\alpha_0 = 1.4$.

4.3. Three-Dimensional Space-Fractional Laplace Case

To assess the numerical effectiveness, a three-dimensional fourth-order equation is considered with a cubic nonlinear term.

$$\begin{aligned}
 & {}_0^c \mathcal{D}_t^{\alpha(t)} (1 + (-\Delta)^s(x, y, z, t)) + A(x, y, t)((-\Delta)^s - \Delta)u(x, y, z, t) \\
 & = u^3(x, y, z, t) - u(x, y, z, t) + f(x, y, z, t), (x, y, z) \in (0, 1)^3, t \in (0, 1], \\
 & u(\Gamma, 0) = 0; u(\partial\Gamma, t) = 0, t \in (0, 1].
 \end{aligned}
 \tag{57}$$

The exact solution of the system is

$$u(x, y, z, t) = \frac{t^3}{3} \sin(\pi x) \sin(\pi y) \sin(\pi z).
 \tag{58}$$

Table 3 provides numerical results for the maximum errors and the corresponding spatial convergence order for various spatial mesh sizes with $h = 1/64$ at $t = 1$. From these results, it can be concluded that the spatial convergence order is close to $O(h^2)$. When $\tau = 1/40$, the accuracy of the two types of maximum errors does not show further improvement. This occurs because the series of maximum errors reaches the upper limit of accuracy of the space discretization.

Table 3. The maximum errors and the corresponding spatial order at $t = 1$ and $h = 1/64$.

τ	1/5	1/10	1/15	1/20	1/30	1/40
s = 0.3						
Error	0.0030	6.9817×10^{-4}	2.8642×10^{-4}	1.7173×10^{-4}	7.3608×10^{-5}	8.8225×10^{-5}
Order		2.1033	2.1975	1.7781	2.0894	-0.6296
s = 0.7						
Error	0.0029	8.4384×10^{-4}	3.4971×10^{-4}	1.6787×10^{-4}	6.7312×10^{-5}	7.9198×10^{-5}
Order		1.7810	2.1725	2.5511	2.2538	-0.5653

5. Conclusions

In this paper, a compact finite difference scheme method using the Picard integral formulation is presented for solving the multi-dimensional time-space fractional partial differential system with a variable order and different nonlinear terms. In contrast to many other schemes, the proposed method takes into account the regularity of the derivative term v . Detailed proofs establish the stability and solvability of this present scheme. To validate the practicality and accuracy of this compact scheme, three numerical experiments are computed and analyzed in different dimensional spatial domains. The numerical results show that the convergence rate aligns with the theoretical value of $O(\tau^2 + h^2)$ in L_∞ norm.

Author Contributions: Conceptualization, S.Y. and C.W.; methodology, S.Y.; software, C.W.; validation, S.Y.; formal analysis, S.Y.; investigation, S.Y.; resources, C.W.; data curation, C.W.; writing—original draft preparation, S.Y.; writing—review and editing, S.Y.; visualization, C.W.; supervision, S.Y.; project administration, S.Y.; funding acquisition, S.Y. All authors have read and agreed to the published version of the manuscript.

Funding: This research was funded by National Treasury-High Level University Summit Program-Existing Master’s Degree Programs in the School of Science (Applied Statistics) grant number 1004892301-40 and the APC was funded by 1004892301-40.

Data Availability Statement: No new data were created or analysed in this study. Data sharing is not applicable to this article.

Acknowledgments: The authors would like to thank the referees for their useful suggestions, which have significantly improved the paper.

Conflicts of Interest: Author Shichao Yi is affiliated with the Yangzijiang Shipbuilding Group. The authors declare that the research was conducted in the absence of any commercial or financial relationships that could be construed as a potential conflict of interest.

References

1. Podlubny, I. *Fractional Differential Equations*; Academic Press: New York, NY, USA, 1999.
2. Kilbas, A.A.; Srivastava, H.M.; Trujillo, J.J. *Theory and Applications of Fractional Differential Equations*; North-Holland: New York, NY, USA, 2006.
3. Baleanu, D.; Diethelm, K.; Scalas, E.; Trujillo, J.J. *Fractional Calculus Models and Numerical Methods*; Series on Complexity, Nonlinearity and Chaos; World Scientific: Boston, MA, USA, 2012.
4. Sun, H.; Zhang, Y.; Baleanu, D.; Chen, W.; Chen, Y. A new collection of real world applications of fractional calculus in science and engineering. *Commun. Nonlinear Sci. Numer. Simul.* **2018**, *64*, 213–231. [[CrossRef](#)]
5. Li, X.; Xu, C. A space–time spectral method for the time fractional diffusion equation. *SIAM J. Numer. Anal.* **2009**, *47*, 2108–2131. [[CrossRef](#)]
6. Zhao, J.; Xiao, J.; Xu, Y. Stability and convergence of an effective finite element method for multiterm fractional partial differential equations. *Abstr. Appl. Anal.* **2013**, *2013*, 857205. [[CrossRef](#)]
7. Zhuang, P.; Gu, Y.T.; Liu, F.; Turner, I.; Yarlagadda, P.K.D.V. Time-dependent fractional advection–diffusion equations by an implicit MLS meshless method. *Int. J. Numer. Methods Eng.* **2011**, *88*, 1346–1362. [[CrossRef](#)]
8. Li, C.; Zhao, Z.; Chen, Y. Numerical approximation of nonlinear fractional differential equations with subdiffusion and super diffusion. *Comput. Math. Appl.* **2011**, *62*, 855–875. [[CrossRef](#)]
9. Liu, F.; Zhuang, P.; Anh, V.; Turner, I. A fractional-order implicit difference approximation for the space time fractional diffusion equation. *ANZIAM J.* **2006**, *47*, 48–68. [[CrossRef](#)]
10. Zhao, Z.; Li, C. Fractional difference/finite element approximation for the time–space fractional telegraph equation. *J. Appl. Math. Comput.* **2012**, *219*, 2975–2988. [[CrossRef](#)]
11. Yi, S.C.; Yao, L.Q. A steady barycentric lagrange interpolation method for the 2d higher order time-fractional telegraph equation with nonlocal boundary condition with error analysis. *Numer. Methods Partial. Differ. Equ.* **2019**, *35*, 1694–1716. [[CrossRef](#)]
12. Chen, W.; Sun, H.; Zhang, X.; Korošak, D. Anomalous diffusion modeling by fractal and fractional derivatives. *J. Comput. Math. Appl.* **2010**, *59*, 1754–1758. [[CrossRef](#)]
13. Inc, M. The approximate and exact solutions of the space- and time-fractional Burgers equations with initial conditions by variational iteration method. *J. Math. Anal. Appl.* **2008**, *345*, 476–484. [[CrossRef](#)]
14. Abdel-Rehim, E.A. Implicit difference scheme of the space–time fractional advection–diffusion equation. *Fract. Calc. Appl. Anal.* **2015**, *59*, 1452–1469. [[CrossRef](#)]
15. Arshad, S.; Huang, J.F.; Khaliq, A.Q.M.; Tang, Y.F. Trapezoidal scheme for time–space fractional diffusion equation with Riesz derivative. *J. Comput. Math. Phys.* **2017**, *390*, 1–15. [[CrossRef](#)]
16. Bhrawy, A.H.; Zaky, M.A. An improved collocation method for multi-dimensional space–time variable-order fractional Schrödinger equations. *Appl. Numer. Math.* **2010**, *59*, 1754–1758.
17. Duo, S.W.; Ju, L.L.; Zhang, Y.Z. A fast algorithm for solving the space–time fractional diffusion equation. *Comput. Math. Appl.* **2018**, *75*, 1929–1941. [[CrossRef](#)]
18. Nie, S.; Sun, H.; Zhang, Y.; Chen, D.; Chen, W.; Chen, L.; Schaefer, S. Vertical Distribution of Suspended Sediment under Steady Flow: Existing Theories and Fractional Derivative Model. *Discret. Dyn. Nat. Soc.* **2017**, *2017*, 5481531. [[CrossRef](#)]
19. Gu, X.M.; Sun, H.W.; Zhao, Y.L.; Zheng, X. An implicit difference scheme for time-fractional diffusion equations with a time-invariant type variable order. *Appl. Math. Lett.* **2021**, *120*, 107270. [[CrossRef](#)]
20. Gu, X.M.; Huang, T.Z.; Ji, C.C.; Carpentieri, B.; Alikhanov, A.A. Fast iterative method with a second order implicit difference scheme for time–space fractional convection–diffusion equations. *J. Sci. Comput.* **2016**, *72*, 957–985. [[CrossRef](#)]
21. Li, M.; Gu, X.M.; Huang, C.; Fei, M.; Zhang, G. A fast linearized conservative finite element method for the strongly coupled nonlinear fractional Schrödinger equations. *J. Comput. Phys.* **2018**, *358*, 256–282. [[CrossRef](#)]
22. Yi, S.C.; Sun, H.G. A Hybridized Trapezoidal-Difference Scheme for Nonlinear Time-Fractional Fourth-Order Advection-Dispersion Equation Based on Chebyshev Spectral Collocation Method. *Adv. Appl. Math. Mech.* **2019**, *11*, 197–215.

Disclaimer/Publisher’s Note: The statements, opinions and data contained in all publications are solely those of the individual author(s) and contributor(s) and not of MDPI and/or the editor(s). MDPI and/or the editor(s) disclaim responsibility for any injury to people or property resulting from any ideas, methods, instructions or products referred to in the content.